Supporting Information

of

Near-Infrared Light Responsive Nanoreactor for Simultaneous Tumor Photothermal Therapy and Carbon Monoxide-Mediated Anti-Inflammation

Shi-Bo Wang,[†,‡,#] *Cheng Zhang*,[†,#] *Jing-Jie Ye*,[†] *Mei-Zhen Zou*,[†,‡] *Chuan-Jun Liu*,[†] and *Xian-Zheng Zhang**,[†,‡]

[†] Key Laboratory of Biomedical Polymers of Ministry of Education & Department of Chemistry, Wuhan University, Wuhan 430072, P. R. China

[‡] Institute for Advanced Studies (IAS), Wuhan University, Wuhan 430072, P. R. China

*Corresponding author: xz-zhang@whu.edu.cn

[#] S.-B.W. and C.Z. contributed equally.

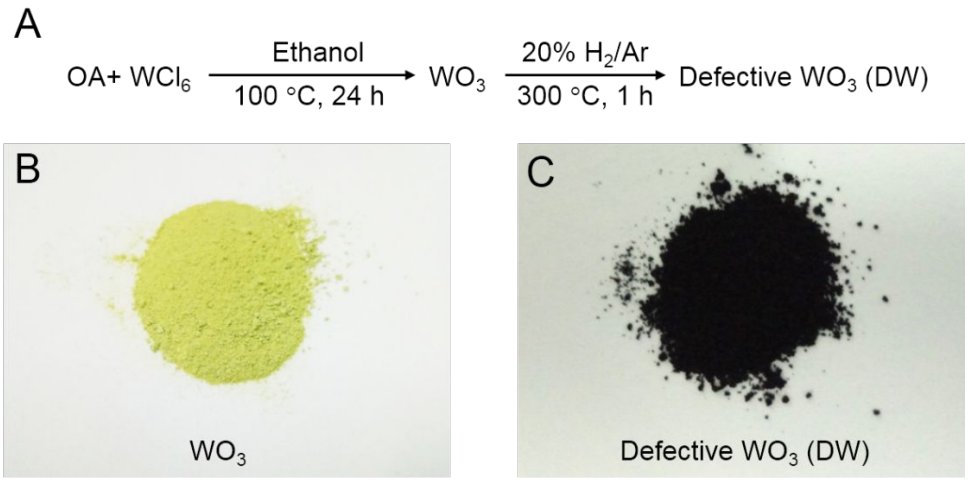

Figure S1. (A) Preparation of DW atomic layers. Photograph of (B) WO_3 atomic layers and (C) DW atomic layers.

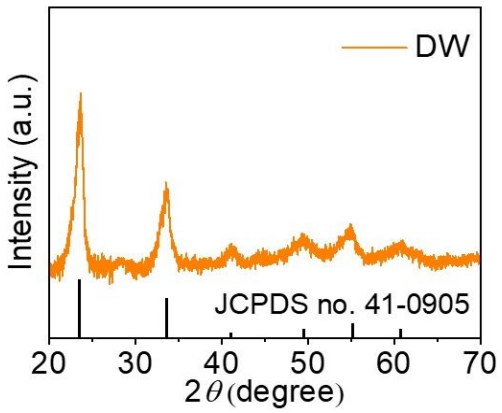

Figure S2. PXRD pattern of DW NSs and JCPDS card of cubic WO_3.

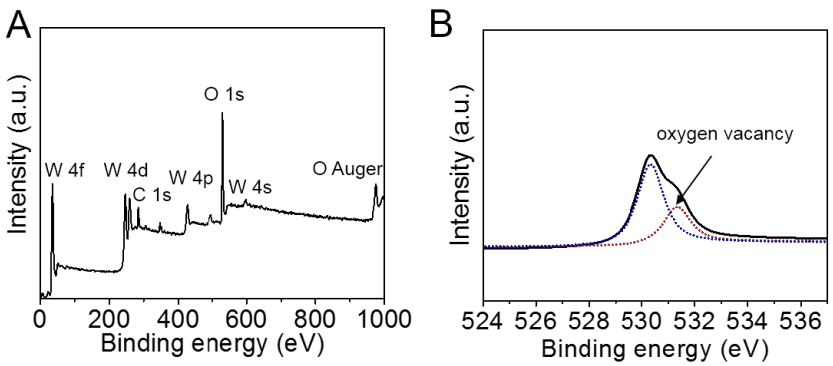

Figure S3. (A) XPS spectrum for DW NSs. (B) O 1s XPS spectrum for DW NSs. The atomic ratio of oxygen vacancies and oxygen atoms was calculated to be 14.7%.

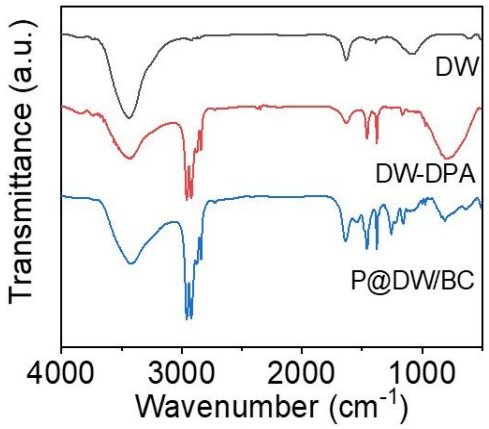

Figure S4. FTIR spectra for DW NSs, DW-PDA NSs, and P@DW/BC NSs.

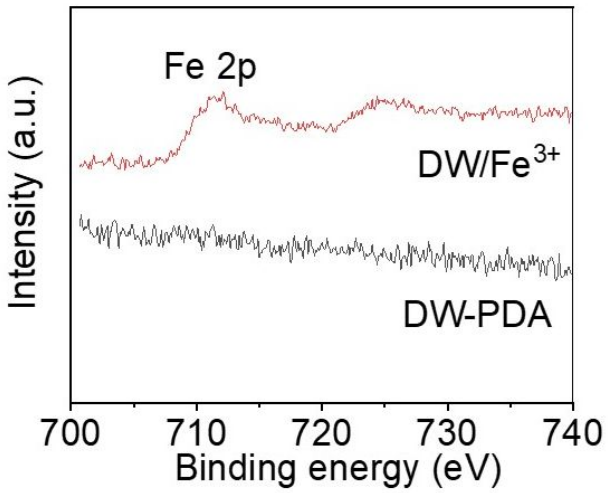

Figure S5. Fe 2p XPS spectrum for DW-PDA and DW/Fe^{3+} NSs.

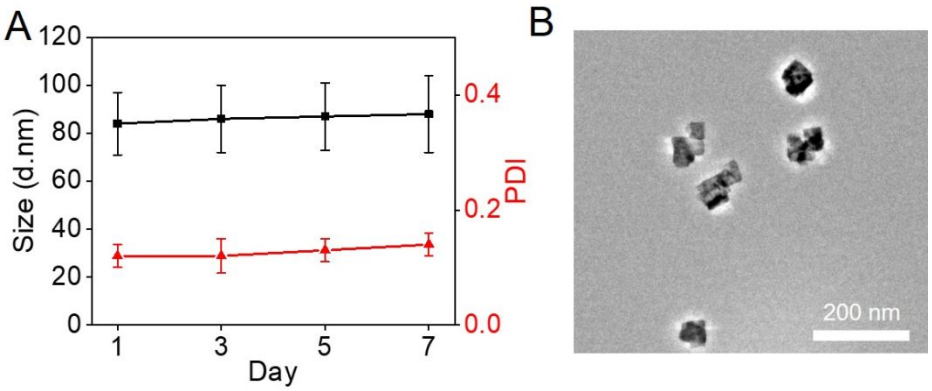

Figure S6. (A) Size distribution and PDI of P@DW/BC NSs in PBS (pH 7.4, 37 °C) for 7 days. (B) TEM image of P@DW/BC NSs after incubated with PBS (pH 7.4, 37 °C) for 7 days.

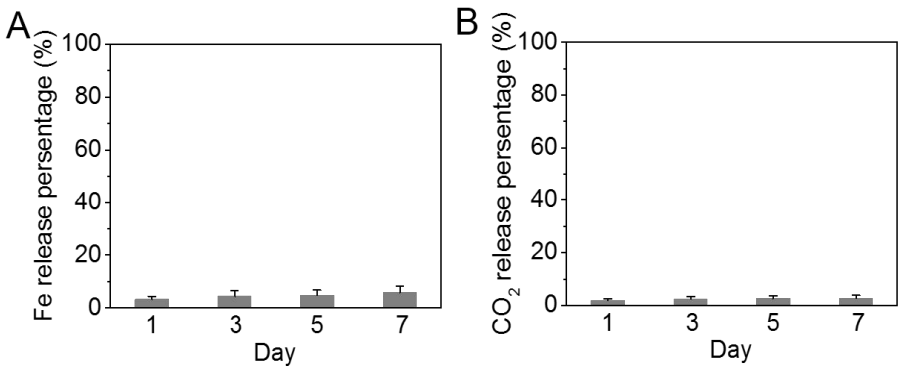

Figure S7. Release amount of (A) Fe^{3+} and (B) CO_2 from P@DW/BC NSs in PBS (pH 7.4) at 37 °C.

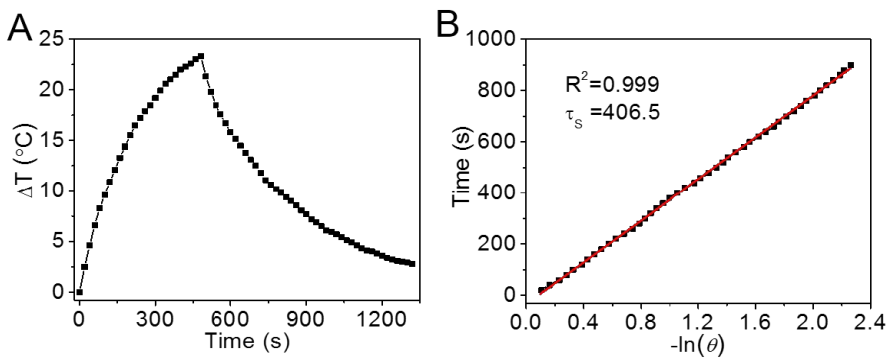

Figure S8. (A) Heating/Cooling experiment of P@DW/BC aqueous solution (200 μg mL^{-1}) under 808 nm laser irradiation (1.5 W cm^{-2}). (B) The cooling time verses -ln(θ).

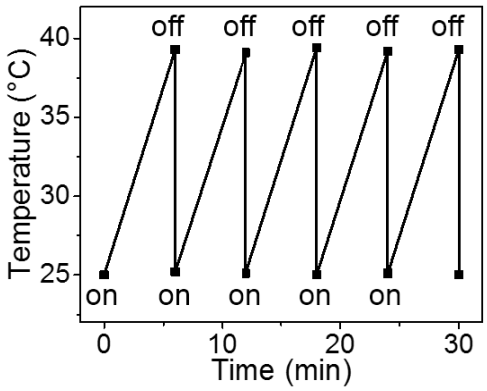

Figure S9. (A) Temperature changes of P@DW/BC solution (100 μg mL^{-1}) over 5 cycles of irradiation/cooling (power density: 1 W cm^{-2}).

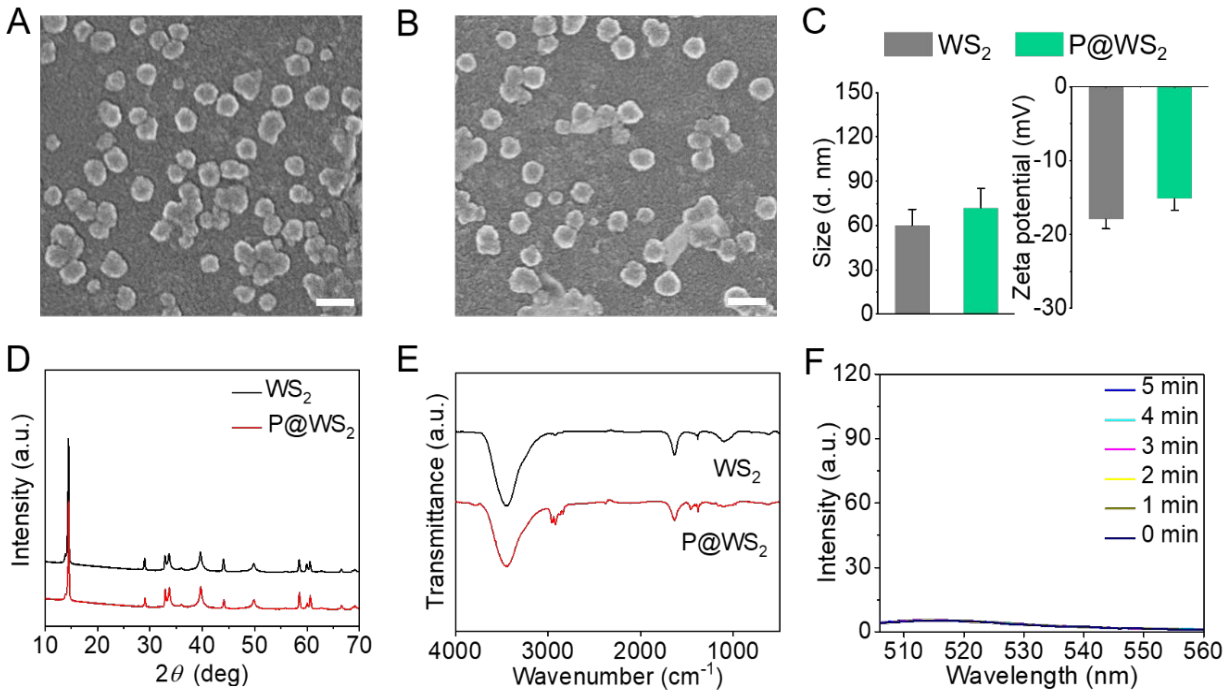

Figure S10. SEM images for (A) WS_2 NSs and (B) $P@WS_2$ NSs. Scale bar: 100 μm. (C) Size distribution and zeta potential of WS_2 and $P@WS_2$ NSs. (D) XRD patterns for WS_2 and $P@WS_2$ NSs. (E) FTIR spectra for WS_2 and $P@WS_2$ NSs. (F) CO generation detection of $P@WS_2$ NSs (200 μg mL^{-1}) under 808 nm laser irradiation (1 W cm^{-2}) by the CO probe.

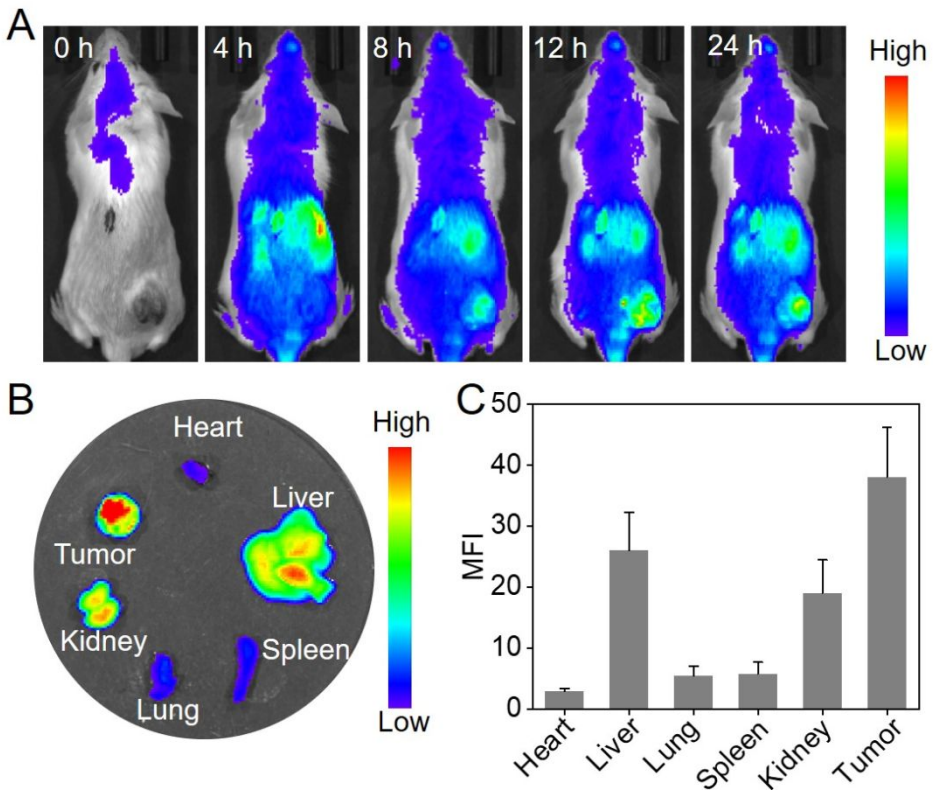

Figure S11. (A) *In vivo*fluorescence imaging of Cy5.5-modified P@DW/BC NSs after intravenous injection. (B) *Ex vivo* fluorescence images of tumor and major organs at 24 h post injection. (C) Quantification of fluorescence intensity of tumor and major organs.

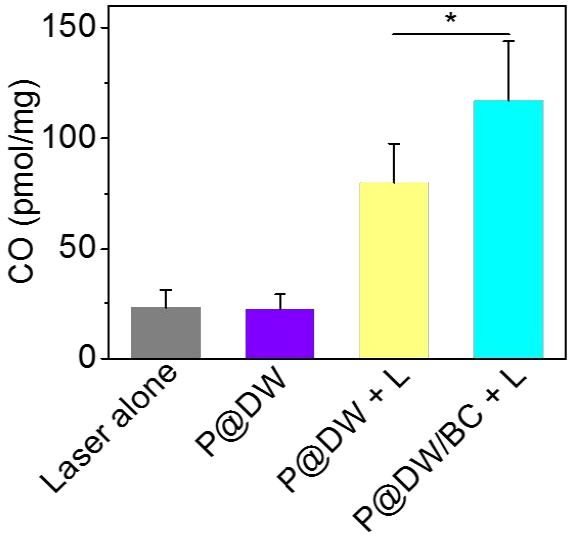

Figure S12. CO contents in tumor tissues of mice treated with laser alone, P@DW, P@DW + L, and P@DW/BC + L. 100 μL of P@DW NSs (10 mg mL^{-1}) were injected to each mouse. $n = 3$, $^*p < 0.05$.

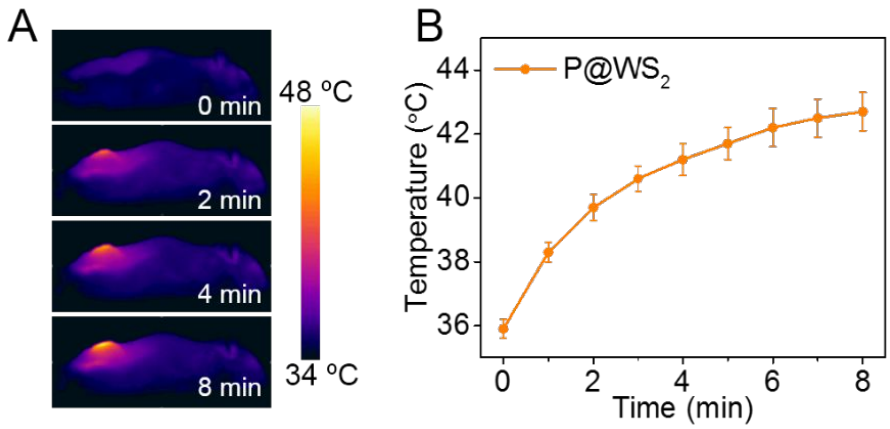

Figure S13. (A) *In vivo* IR thermal imaging of mice treated with P@WS_2 NSs (100 μL per mouse, 9 mg mL^{-1}) under 808 nm laser irradiation (1 W cm^{-2}). (B)Temperature changes of tumor tissues during the irradiation. The dosage of P@WS_2 NSs for each mouse was controlled to result in nearly the same *in vivo* photothermal effect as P@DW/BC NSs (100 μL per mouse, 10 mg mL^{-1}).

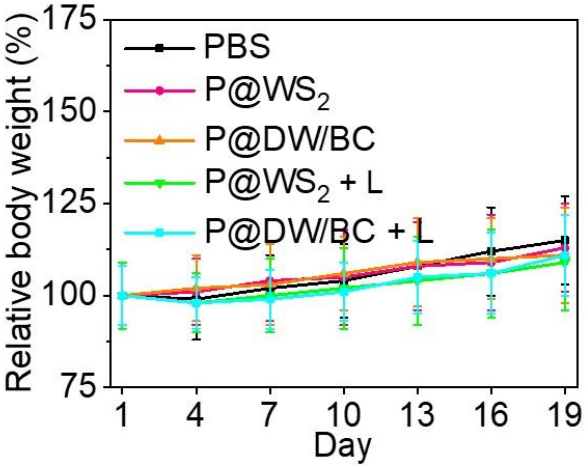

Figure S14. Relative body weight of mice from different groups during the treatments.

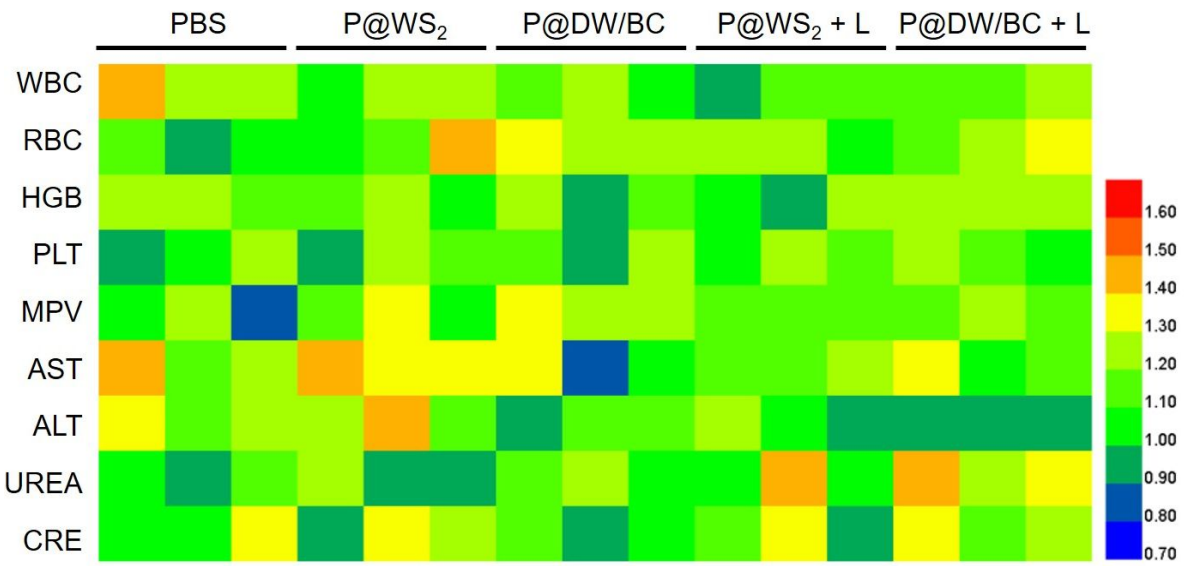

Figure S15. Blood biochemistry analyses of mice from different groups on the 19th day.

The results were shown as the relative intensity of the indexes.

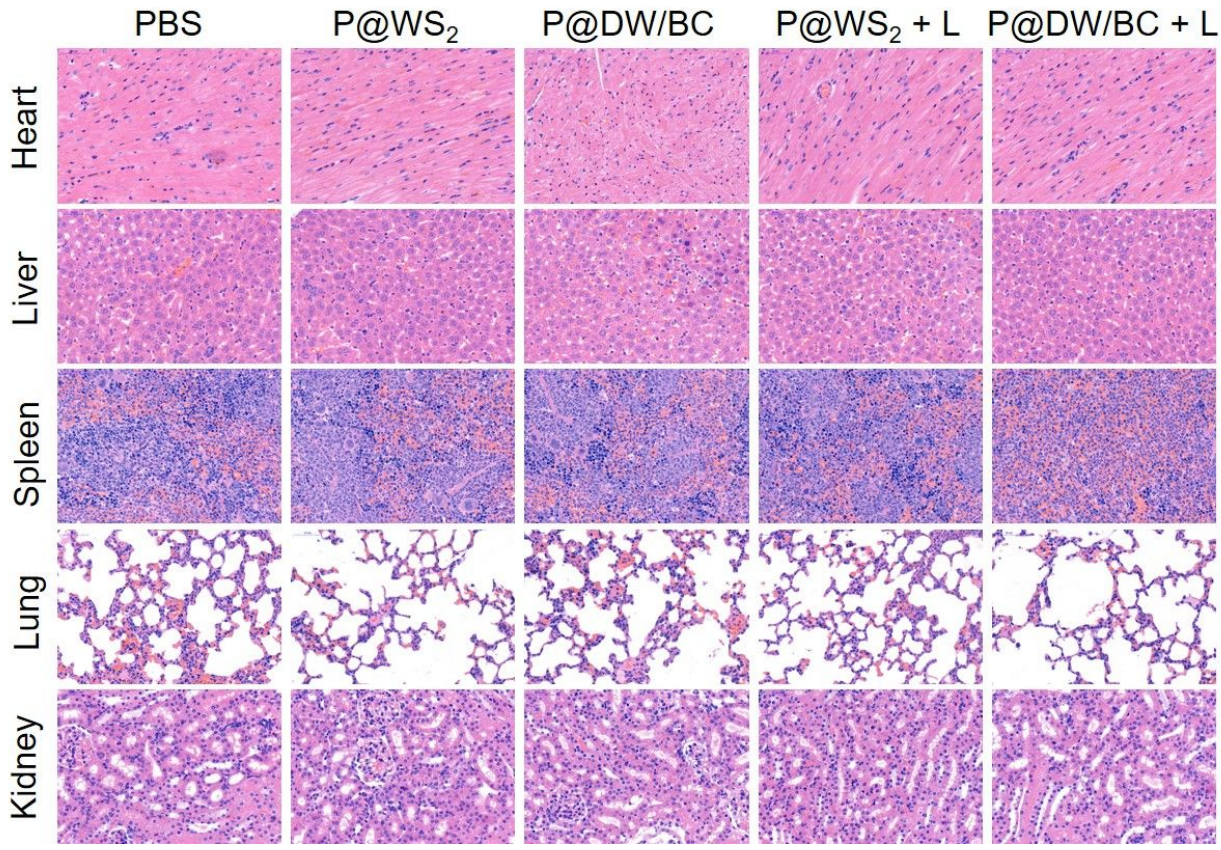

Figure S16. H&E staining pictures of major organs of mice from different groups on the 19th day (×40).

Table 1. Photothermal conversion efficiency of some representative PTAs.

PTAs	Photothermal conversion efficiency (%)	References
Graphene oxide	25	*Chem. Commun.* **2014**,*50*, 14345
MoS_2 NSs	24	*ACS Nano.* **2014**, *8*, 6922
Black phosphorus quantum dots	28.4	*Angew. Chem. Int., Ed.* **2015**, *54*, 11526
PEG-TaS_2 NSs	39	*Adv. Funct. Mater.* **2017**, *27*, 1703261
WS_2 quantum dots	44.3	*ACS Nano.* **2015**, *9*, 12451
Antimonene quantum dots	45.5	*Angew. Chem. Int., Ed.* **2017**, *56*, 11896